

Signatures of Coherent Electronic Quasiparticles in the Paramagnetic Mott Insulator.

Mats Granath¹ and Johan Schött²

¹*Department of Physics, University of Gothenburg, SE-41296 Gothenburg, Sweden and*

²*Department of Physics and Astronomy, Uppsala University, P.O. Box 516, SE-751 20 Uppsala, Sweden*

(Dated: 24 augusti 2021)

We study the Mott insulating state of the half-filled paramagnetic Hubbard model within dynamical mean field theory using a recently formulated stochastic and non-perturbative quantum impurity solver. The method is based on calculating the impurity self energy as a sample average over a representative distribution of impurity models solved by exact diagonalization. Due to the natural parallelization of the method, millions of poles are readily generated for the self energy which allows to work with very small pole-broadening η . Solutions at small and large η are qualitatively different; solutions at large η show featureless Hubbard bands whereas solutions at small $\eta \leq 0.001$ (in units of half bare band width) show a band of electronic quasiparticles with very small quasiparticle weight at the inner edge of the Hubbard bands. The validity of the results are supported by agreement within statistical error $\sigma_{\text{QMC}} \sim 10^{-4}$ on the imaginary frequency axis with calculations using a continuous time quantum Monte Carlo solver. Nevertheless, convergence with respect to finite size of the stochastic exact diagonalization solver remains to be rigorously established.

PACS numbers: 74.25.Ha, 74.25.Jb, 74.72.-h, 79.60.-i

The concept of electronic quasiparticles is one of the most basic paradigms in the description of the dense interacting electron system found in any metallic atomic crystal. In terms of quasiparticles even superficially very strongly interacting systems may be described through elementary excitations that are in direct correspondence with those of a non-interacting electron gas. This allows for a relatively simple description of thermodynamic and transport properties, as well as the inclusion of interactions between quasiparticles and phonons which is the basis of the standard theory of superconductivity as a condensate of paired quasiparticles.

The basic theory of quasiparticles is well understood within the framework of quantum many particle physics¹ where the distribution of single electron excitations at (crystal) momentum \vec{k} and energy ω ($\hbar = 1$) are described by the spectral function $A_{\vec{k}}(\omega)$. The object that captures the effects of interactions is the self energy $\Sigma_{\vec{k}}(\omega)$ in terms of which the spectral function can be expressed as $A_{\vec{k}}(\omega) = -\frac{1}{\pi} \frac{\text{Im}\Sigma_{\vec{k}}(\omega)}{(\omega - \epsilon_{\vec{k}} + \mu - \text{Re}\Sigma_{\vec{k}}(\omega))^2 + (\text{Im}\Sigma_{\vec{k}}(\omega))^2}$. Here $\epsilon_{\vec{k}}$ is the bare band energy of the system and μ is the chemical potential and we have assumed a single band which is isolated from any other effects than those of intraband electron-electron interactions. In a Fermi liquid the quasiparticles are objects that close to the Fermi energy, at energy $\omega = E_{\vec{k}}$ solves $\omega - \epsilon_{\vec{k}} + \mu - \text{Re}\Sigma_{\vec{k}}(\omega) = 0$. These are characterized by a lifetime $\tau^{-1} = -2\text{Im}\Sigma_{\vec{k}}(\omega = E_{\vec{k}})$, quasiparticle weight $Z_{\vec{k}}^{-1} = 1 - \partial_{\omega}\text{Re}\Sigma_{\vec{k}}(\omega)|_{E_{\vec{k}}}$, and effective mass. The quasiparticle weight $Z_{\vec{k}}$ quantifies how much of the spectral weight at momentum \vec{k} is carried by the Landau quasiparticle and will be manifest as the characteristic discontinuity at $T = 0$ in the occupation number $n_{\vec{k}} = \int_{-\infty}^0 d\omega A_{\vec{k}}(\omega)$ which defines the Fermi surface.

For an interacting electron system it can be understood in perturbation theory how the quasiparticles are a con-

sequence of phase space constraints for scattering which gives a vanishing $\text{Im}\Sigma(\omega = 0) = 0$ and a correspondingly divergent lifetime of quasiparticles at the Fermi energy.¹

In contrast a Mott insulator is a system that from the band structure considerations would be a metal but which has been driven insulating by electron-electron interactions.² The defining feature of the insulator is exactly that there are no low energy electronic quasiparticles, instead there is a gap in the spectral function around the Fermi energy. In its cleanest form (without broken translational symmetry) the Mott insulator is a non-Fermi liquid in the sense that the self energy diverges at small ω , and electronic quasiparticles are thus always unexpected. Quasiparticles, if found, would be of fundamental importance and might also provide a setting for theories of more exotic states in strongly correlated systems.

In this paper we study the Mott insulator in infinite dimensions within dynamical mean field theory (DMFT)³⁻⁷, for the standard case of the single band paramagnetic Hubbard model with a semi-circular density of states. Although this is a much studied⁸⁻¹⁷ and by now perhaps the archetypical model of a Mott insulator (and Mott transition), we have found evidence that a basic feature of the spectral function may be missing in most earlier studies; namely that it may contain well defined electronic quasiparticles at the gap edge. We have used a stochastic non-perturbative method, "distributional exact diagonalization" (Dist-ED)¹⁶ which can give exceptionally high resolution of the self energy over the full band width. The method in brief consists of calculating the self energy of the DMFT (Anderson) impurity problem as a sample average over representative but stochastically generated finite size impurity models that are solved by exact diagonalization. In standard fashion a finite shift $\eta > 0$ away from the real axis is used in order to generate a continuous function from a finite set

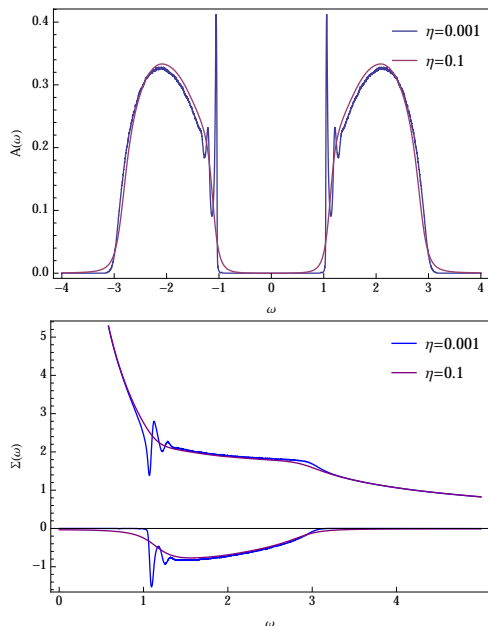


Figure 1: Converged solutions at $U = 4$ ($n_s = 5$) for large ($\eta = 0.1$) and small ($\eta = 0.001$) broadening, showing the upper and lower Hubbard bands as well as the very sharp peak at the inner edge. (Bottom) Corresponding real and imaginary parts of the self energy. (The pole at $\omega = 0$ is not shown in $Im\Sigma$.) The $\eta = 0.001$ calculation is an average of $6 \cdot 10^6$ samples with a corresponding self energy consisting of $> 10^8$ poles.

of poles, but due to the natural parallelization of the present method, millions or even billions of poles can be generated which allows for the use of very small η . Quasiparticles are found only at $\eta \leq 0.001$ (in units of half bare band width) and for not too large U , suggesting that both of these aspects, non-perturbative and high resolution, are crucial to the result. In order to see this feature it is thus necessary to be able solve the DMFT equations non-perturbatively and very close to the real axis which is difficult with other methods at the high energies related to the Mott gap.

The main result of the paper, as shown in Figure 1, is the sharp peaks in the local density of states and the imaginary part of the self energy for small $\eta = 0.001$ at the inner edge of the Hubbard bands, a feature that is not found for larger $\eta = 0.1$. In Figure 2 it is shown that this edge peak derives from an actual quasiparticle solution $\omega - Re\Sigma - \epsilon = 0$, for a narrow window of ω values and a range of bare band-energies ϵ . The corresponding energy resolved spectral function, $A(\epsilon, \omega) = -\frac{1}{\pi} Im(\frac{1}{w + \mu - \epsilon - \Sigma(\omega)})$, shows narrow dispersing bands (Fig. 3) together with the broad incoherent weight. An important conclusion, as demonstrated in Figures 4 and 5, is that the quasiparticle solutions are only observed if the DMFT self consistency cycle is performed very close to the real axis, and in Figure 7 that the small and large η solutions are qualitatively different. This difference can be linked to a small energy scale (see Figure 9)

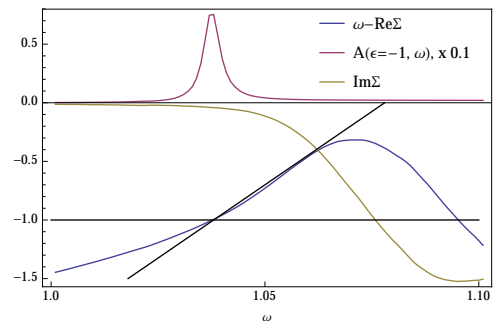


Figure 2: Close-up of the the quasiparticle at $\epsilon = -1$ (not integrated over band energies), together with $Im\Sigma$ and $\omega - Re\Sigma$, showing that this is an actual quasiparticle that solves $\omega - \epsilon - Re\Sigma = 0$ close to the bare band edge $\epsilon = -1$ with a large lifetime $(Im\Sigma)^{-1}$. The tangent at the crossing correspond to the inverse quasiparticle weight $Z^{-1} = 1 - \partial_\omega Re\Sigma \approx 25$.

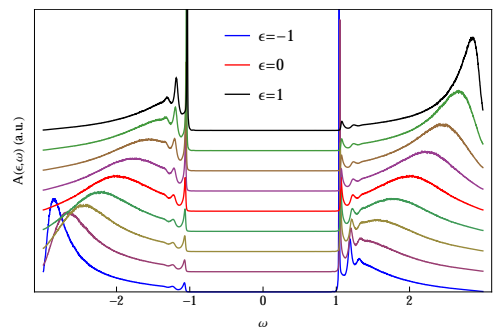


Figure 3: Spectral function $A(\epsilon, \omega)$ resolved with respect to band energy ϵ . Showing the broad incoherent Hubbard bands together with the very narrow band of gap edge quasiparticles.

of separation between spectral weight, $A(\omega)$, and scattering, $Im\Sigma(\omega)$, which is a non-perturbative outcome from exact diagonalization. This energy scale is diminished at large U such that the known strong coupling form¹² (Fig. 8) of the Hubbard bands is asymptotically reached. Comparing to calculations using a continuous time quantum Monte Carlo (CT-QMC) impurity solver²³ (Fig. 10) on imaginary frequencies show that the small η solutions are in agreement within statistical error with the QMC calculations.

Similar sharp peaks as found in our study have been reported before in various forms but are difficult to distinguish from peaks due to finite resolution of poles. In the metallic phase, there is quite strong evidence that such gap edge peaks do appear.^{15,17} Also, in the antiferromagnetic case such features have been observed, where they might (at least physically) be understood in terms of coupling to low energy magnon modes.¹⁹ One study, by Nishimoto et al.¹³ using dynamical density-matrix renormalization group (D-DMRG)²⁰ finds additional peak structure even in the insulating paramagnetic phase, although the details of the self-energy is not explored. As our study is limited to small system sizes with number of levels $n_s = 3, 5$, or 7 , the qualitatively similar results in the D-DMRG study with $n_s \sim \mathcal{O}(200)$ is reassuring.

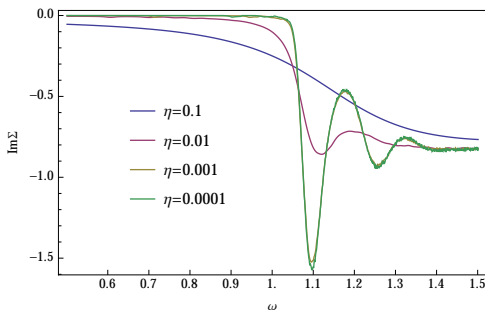


Figure 4: Dependence on η , broadening of poles, for the imaginary part of the self-energy, for $\eta = 10^{-1}, 10^{-2}, 10^{-3}, 10^{-4}$. To resolve any peak structure requires a small $\eta \leq 10^{-2}$, with convergence for $\eta \leq 10^{-3}$.

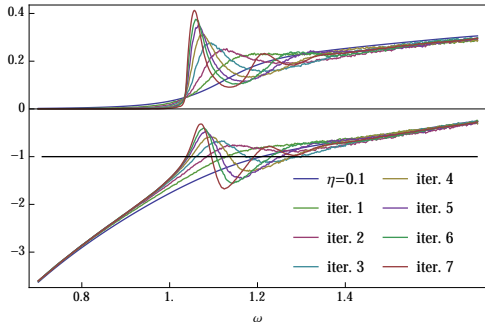


Figure 5: DMFT iterations at $\eta = 0.001$, showing $\omega - \text{Re}\Sigma(\omega)$ (lower panel) and corresponding $A(\omega)$, close to inner band edge. The iterations are started from a (featureless) converged solution at $\eta = 0.1$ and show that the quasiparticle peak is not an explicit finite size effect but rather a feature that is iteratively enhanced in the DMFT cycle.

Nevertheless, other more recent studies do not find quasiparticles in the Mott insulating state and it seems fair to say that this is still an open question.^{15,17,18}

Model and method

The model studied is the single band Hubbard model with on-site interaction quantified by U but treated in infinite dimensions where it can be exactly mapped to a quantum impurity with a momentum independent self energy.³ We additionally assume that there is no broken symmetry such that there is no magnetic or charge order.

At half-filling, $\mu = U/2$, and using a semi-circular bare density of states $\rho_0(\omega) = \frac{2}{\pi}\sqrt{1-\epsilon^2}$ ($|\epsilon| \leq 1$) of bandwidth 2, the local interacting Greens function (for one spin species) is $G(z) = \int d\epsilon \frac{\rho_0(\epsilon)}{z + \mu - \epsilon - \Sigma[G](z)}$, which can be integrated to the form

$$G(z) = \frac{1}{z + \mu - \Delta[G](z) - \Sigma[G](z)}, \quad (1)$$

with $\Delta[G] = (1/4)G$. Here $\Sigma[G]$ is the self energy of the corresponding Anderson impurity specified by interaction U and chemical potential μ on the impurity site, and hybridization between impurity and continuum $\Delta[G]$. The

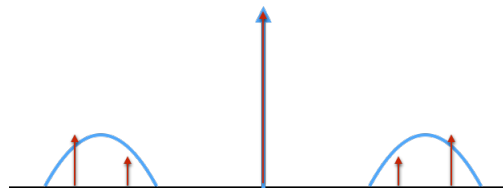


Figure 6: Schematic of the sampling of the continuous impurity-bath Greens function $G_0 = \frac{a_0}{z} + g_0(z)$ in terms of a five level ($n_s = 5$) system $G_0^\nu = \frac{a_0}{z} + \sum_{i=1}^4 \frac{a_i^\nu}{z - b_i^\nu}$. The location of the satellite poles at finite ω are generated stochastically based on the distribution $-Img_0(\omega)$ with random (normalized) residues.

challenging task is to solve for the self energy, or equivalently, the interacting Green's function of the impurity model.

The standard diagrammatic perturbation theory would involve the impurity-bath Greens function $G_0(z) = \frac{1}{z - \Delta}$ as propagators with four point vertex U and two-point vertex μ . (As discussed shortly the inclusion of μ in the interaction rather than the propagator is in principle a matter of convenience.) We will not do perturbation theory but nevertheless use G_0 (rather than Δ) to describe the impurity. Assuming Δ is particle-hole symmetric and with a clean gap we can write

$$G_0 = \frac{a_0}{z} + g_0(z), \quad (2)$$

with $a_0 = (1 - d_\omega \Delta|_{\omega=0})^{-1}$. Here g_0 is gapped such that $Img_0(\omega + i0^+) = 0$ for $|\omega| < \epsilon_{gap}$ and has integrated weight $\int d\omega \frac{-1}{\pi} Img_0(\omega) = 1 - a_0$.

The choice of including the chemical potential in the interaction rather than in the non-interacting Greens function ($G'_0 = 1/(z + \mu - \Delta)$) is convenient (and standard for this problem) because it makes G_0 particle-hole symmetric. Within the present approximation the convention is also valuable because it isolates a substantial part of the spectral weight in a single pole at $\omega = 0$ that may be represented exactly by a finite system, and it also separates the pole from the continuum with a gap of finite width.

As was suggested in Ref. 16 and presently specialized to the *gapped* Anderson model we propose to make an approximate calculation of the self energy in the following way:

1) Generate a large number N of finite-size Anderson models (see Fig. 6) indexed by $\nu = 1, \dots, N$ with n_s orbitals (n_s odd) that correspond to a finite impurity-bath Greens function

$$G_0^\nu = \frac{a_0}{z} + \sum_{i=1}^{n_s-1} \frac{a_i^\nu}{z - b_i^\nu}. \quad (3)$$

For $i < n_s/2$ the pole locations b_i^ν are picked using g_0 as a probability distribution function, such that

$$P(b_i^\nu) = -\frac{1}{(1 - a_0)\pi} Img_0(\omega = b_i^\nu + i0^+), \quad (4)$$

and a_i^ν is a random positive number. Particle-hole symmetry is enforced by taking $b_i^\nu = -b_{n_s-i}^\nu$ and $a_i^\nu = a_{n_s-i}^\nu$ for $i > n_s/2$, and normalization by taking $\sum_{i=1}^{n_s-1} a_i^\nu = 1 - a_0$. The construction ensures that

$$\langle G_0^\nu \rangle \equiv \lim_{N \rightarrow \infty} \frac{1}{N} G_0^\nu = G_0. \quad (5)$$

2) Identify parameters of the Anderson Hamiltonian

$$H^\nu = U n_{0,\uparrow} n_{0,\downarrow} - \mu n_0 - \sum_{i=1, \sigma}^{n_s-1} V_i^\nu (c_{i\sigma}^\dagger c_{0,\sigma} + \text{h.c.}) + \sum_{i=1}^{n_s-1} \epsilon_i^\nu n_i \quad (6)$$

where $n_{i\sigma} = c_{i\sigma}^\dagger c_{i\sigma}$ is the number operator at the bath site $i > 0$ or impurity site $i = 0$ with spin $\sigma = \uparrow, \downarrow$ and n_i is summed over spin. Hopping between impurity and bath site i is given by V_i^ν and the bath level energy by ϵ_i^ν . The non-interacting part of the hamiltonian corresponds to the equivalent form of the Greens function

$$G_0^\nu = \frac{1}{z - \sum_{i=1}^{n_s-1} \frac{(V_i^\nu)^2}{z - \epsilon_i^\nu}} \quad (7)$$

which allows for an exact mapping of parameters $\{a_i^\nu, b_i^\nu\} \rightarrow \{V_i^\nu, \epsilon_i^\nu\}$, through the location $G_0^\nu(\omega)|_{\omega=\epsilon_i} = 0$ and derivative $V_i^\nu = (-d_\omega G_0^\nu|_{\epsilon_i})^{-1/2}$ of roots on the real axis.

3) Calculate, using exact diagonalization, the interacting Greens function G^ν and the corresponding self energy

$$\Sigma^\nu(z) - \mu = (G_0^\nu)^{-1} - (G^\nu)^{-1}. \quad (8)$$

To be very confident of the accuracy we have calculated G^ν as an explicit sum over all poles that correspond to single particle excitations from the ground states,

$$G^\nu(z) = \frac{1}{2} \sum_{s=\uparrow, \downarrow; m} \left(\frac{\langle m | c_{0,\uparrow}^\dagger | 0, s \rangle^2}{z - (E_m - E_0)} + \frac{\langle m | c_{0,\uparrow} | 0, s \rangle^2}{z + (E_m - E_0)} \right) \quad (9)$$

A block diagonal form in particle number n , spin S and S^z in which the degenerate ground states are known to be in sectors $n = n_s$, $S = 1/2$ and $S^z = \pm 1/2$ is used. The self energy $\Sigma^\nu(\omega)$ is then calculated by inverting the Greens function away from the real axis at $\omega + i\eta$. The latter with the exception of the pole at $\omega = 0$ that we calculate explicitly as $\alpha^\nu = -\frac{1}{\partial_\omega G^\nu|_{\omega=0}}$. (Removing numerically the corresponding contribution in the inverted Greens function.) At this point the self-energy can also be readily evaluated at any point z away from the real axis for comparison with QMC results on Matsubara frequencies.

4) Calculate the self energy as

$$\Sigma(\omega) = \langle \Sigma^\nu(\omega) \rangle \equiv \frac{1}{N} \sum_{\nu=1}^N \Sigma^\nu(\omega), \quad (10)$$

with the pole at $\omega = 0$ given explicitly by $\alpha = \frac{1}{N} \sum_\nu \alpha^\nu$. As emphasized in Ref. 16 it is *not* appropriate to calculate the self energy as $\Sigma' - \mu = \langle G_0^\nu \rangle^{-1} - \langle G^\nu \rangle^{-1}$, because the mean of the Greens functions do not satisfy a Dyson equation. The latter implies that roots of G_0 are also roots of G which will not be satisfied for the means.

The calculation of the self energy is the crux of the DMFT iteration, where $\Sigma(\omega)$ is then used to calculate a new impurity-bath Green's function $G_0(\omega)$. The pole strength at $\omega = 0$ is given exactly by $a_0 = 1/(1 + \frac{1}{4\alpha})$, making it convenient (but not crucial for the results) to keep track of this explicitly. Importantly, the broadening η is built into the cycle, as the starting point of the next iteration is based on an assumed real frequency Greens function which is actually calculated from a self energy evaluated a finite distance from the real axis. Thus, even if at each iteration the dependence on η may be quite weak, the difference will be iteratively enhanced such that the self consistent solutions for small and large η turn out radically different.

Results and discussion

We have done calculations using $n_s = 3, 5$, and 7 for U ranging from close to $U_{c1} \approx 2.5$ to very large, and η ranging from 0.1 down to 10^{-5} . We have focused primarily on $U = 4$, well into the insulating region of the phase diagram, using $n_s = 5$ and $\eta = 0.001$ which are the results discussed and shown in the figures unless stated otherwise. Calculations have been done on a compute cluster using up to 300 kernels, sampling up to $N = 10^7$ 5-level systems which corresponds to a self energy built up of 10^9 poles. This large number of stochastically distributed poles allows for η as small as 10^{-4} without significant noise. We have used a discretization $\Delta\omega = 0.001$, but since the mapping $\Sigma(\omega) \Leftrightarrow G_0(\omega)$ is point for point this does not introduce any additional approximation (unless there is structure on an even smaller scale) even if $\eta < \Delta\omega$. The only consequence is that in the latter case we need to have a very large number of samples N in order to capture the proper $N \rightarrow \infty$ value of Σ . To initialize the calculations we use an arbitrary insulating self energy such as the expression for an isolated site, $\Sigma(z) \sim 1/z$.

The main result of these calculations (Fig. 1) that the self consistent solutions for the self energy and corresponding spectral function has a narrow peak structure at the inner edge of the Hubbard bands. The peak corresponds to an actual narrow band of coherent quasiparticles solving $\omega - \epsilon + \mu - \text{Re}\Sigma(\omega) = 0$ for a range of ω values and that are clearly distinguished from the incoherent weight contributing to the main part of the Hubbard bands. At $U = 4$ we find a quasiparticle weight $Z \approx \frac{1}{25}$. The quasiparticle weight does not appear to be strongly U dependent, instead the quasiparticles are defined over a decreasing fraction of the bare band width with increasing U

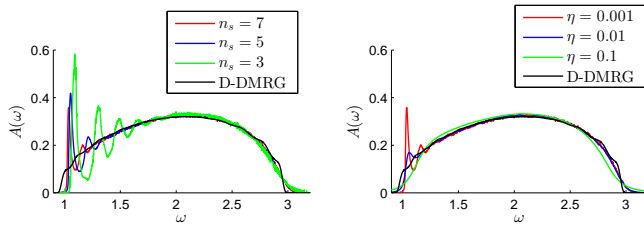


Figure 7: Upper Hubbard band $A(\omega)$, Dist-ED converged at various n_s (with $\eta = 0.001$) and various η (with $n_s = 7$) at $U = 4$ and compared to results using D-DMRG.¹⁵

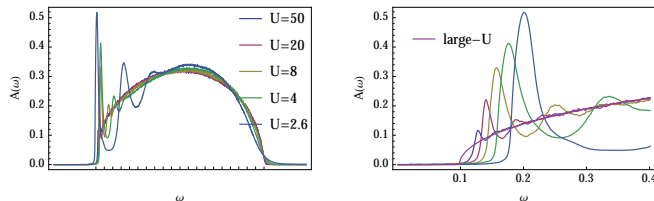


Figure 8: Upper Hubbard band for various $U = 2.6, 4, 8, 20, 50$, shifted to same center (left). Inner edge (right) showing the gradual disappearance (arbitrary offset) of the peak structure for large U and compared to the exact result to lowest order in $1/U$.¹² At the largest U there are no actual quasiparticles.

leading to a gradual disappearance of the peak. Eventually, for large U , there is no quasiparticle solution, but only a remnant peak. There is also weaker more strongly damped (non-quasiparticle) secondary peaks that follow from the coupled oscillations of $G(\omega)$ and $\Sigma(\omega)$ built into the DMFT solution.

A surprising property of the calculations is that solutions are very sensitive to the pole broadening η , with solutions converged at $\eta = 0.1$ have a featureless self energy and spectral weight with no evidence of the quasiparticles that are found at smaller η . Operationally we find that this qualitative difference comes from the fact that the self energy and local Greens function are coupled self consistently which may enhance slight differences. As exemplified in Figure 5, starting a calculation with $\eta = 0.001$ from a converged solution at $\eta = 0.1$ there is at each DMFT iteration only a slight enhancement at the inner edge of band but that eventually develops into the full quasiparticle peak.

Comparing to D-DMRG results by Karski et al.¹⁵ we find that the large η featureless solutions are in good, semi-quantitative, agreement. The lack of quantitative agreement may be due to the additional step of analytic continuation from finite η to real frequency for the D-DMRG results. In contrast, as discussed before, other D-DMRG results by Nishimoto et al. do find a peak structure close to U_{c1} .

At a more basic level we find that we can identify an energy scale that must be resolved in order to find the quasiparticle solution. The quasiparticles that give a peak in $A(\omega)$ are caused by a sharp oscillation in the $Re\Sigma$ which by analyticity precedes (in $|\omega|$) a peak in $Im\Sigma$. This implies that the self-consistent solution must have

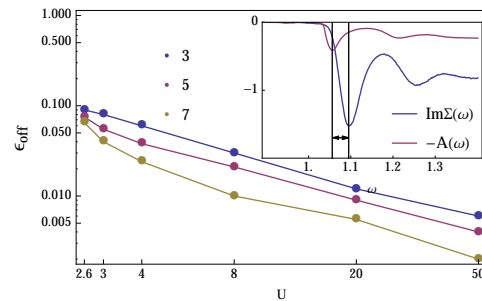


Figure 9: Energy scale ϵ_{off} of separation between the peak in $A(\omega)$ and $Im\Sigma(\omega)$, and dependence on n_s . This energy scale must be well resolved in order to observe the quasiparticles. (The numbers are estimates with accuracy limited primarily by the broadness of the peaks.)

an offset ϵ_{off} between the two peaks (see inset of Fig. 9). This is exactly the outcome of the calculation of the self energy, there is a small U -dependent offset $\epsilon_{\text{off}} \leq 0.1$ between the inner edge of spectral weight (the spectral gap) and the onset of scattering. We observe from solving finite systems, that there is such an offset, poles in Σ^ν (identified as zeroes in G^ν) are always at higher energies than multiples of the bare pole locations of G_0^ν , an effect which seems genuinely non-perturbative. (In perturbation theory we would expect poles in Σ^ν at integer multiples of the poles in the bare greens function G_0^ν .) The crux of the matter is of course whether this offset survives the limit $n_s \rightarrow \infty$. As shown in Figure 9 the energy scale is diminished with n_s , although at the smallest U studied we actually find very little difference between $n_s = 3, 5$, and 7 .

To put this in context, for the metallic solution (not studied here) there is an energy scale related to the width of the central peak in $A(\omega)$ which is actually the Kondo scale, T_K , of the Anderson impurity.^{3,11} The energy scale identified here for the insulator is also related to the width of a (gapped) quasiparticle peak but whether the two energy scales are related in some way remains to be explored. For the metal, T_K vanishes at the metal-insulator transition $U_c \approx 3$, whereas the energy scale ϵ_{off} appears to vanish only asymptotically for large U .

Quantum Monte Carlo calculations for quantum impurities are in principle numerically exact in the limit of large simulation time.^{21,22} Nevertheless, there is at least two major drawbacks of the method which for the Mott insulator studied here makes the method less relevant. First, it works at finite temperature $\beta^{-1} = k_B T > 0$, such that when the gap scale is small there will be appreciable deviations from the $T = 0$ results.

Secondly, and more dramatic, because it is an imaginary time formalism it gives information about the Greens function or self energy on corresponding imaginary (Matsubara) frequencies $i\omega_n = i\frac{\pi}{\beta}(2n + 1)$. To get real frequency information requires an analytic continuation, but with statistical noise for finite simulation times it is not feasible to study structure at high energies on the fine scale discussed in this paper. Nevertheless, a direct

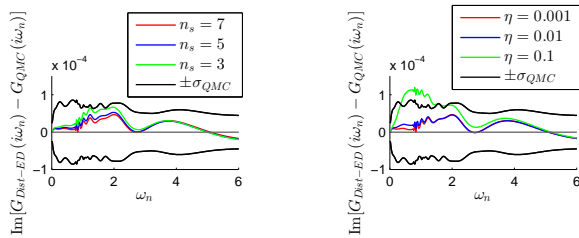


Figure 10: Dist-ED for various various n_s (using $\eta = 0.001$) and various η (using $n_s = 7$), compared to CT-QMC calculations at inverse temperature $\beta = 200$ and $U = 4$ on the Matsubara frequencies $i\omega_n = \frac{\pi}{\beta}(2n + 1)$, with σ_{QMC} the calculated statistical error of the QMC data.

comparison on the Matsubara frequencies of the Dist-ED results (available for any complex frequency) should provide a useful and rigorous test. We have used the TRIQS code²³ and the hybridization expansion routine within continuous time quantum Monte Carlo (CT-QMC).²² Within the limits set by reasonably achievable noise levels, $\sigma_{\text{QMC}} \approx 10^{-4}$, of the CT-QMC we find that the Dist-ED results are in very good agreement with the QMC for all parameter values, which is remarkable given how different the solutions appear over real frequencies (Fig. 7). Only for the large $\eta = 0.1$ solution (featureless on the real axis) does there appear to be a statistically relevant deviation from the QMC data, which may be related to the slightly wider tails of the spectra in this case. Clearly, the gap edge quasiparticles are consistent with QMC on the imaginary axis, but the latter is too insensitive to the details of real frequency structure to provide a very stringent test.

To conclude, we have found evidence that the Mott insulating state of the Hubbard model in infinite dimensions with a semicircular density of states has well defined gapped electronic quasiparticles even in the paramagnetic phase. We have used the method of distributional exact diagonalization¹⁶ in which the impurity self energy of the DMFT impurity model is calculating as a sample average of the exact self energy of a representative distribution of impurities models with n_s levels. Our results suggest that it is crucial to have a very good resolution at each iteration of the DMFT cycle to resolve a small non-perturbatively generated energy scale. We speculate that the quantitative details of the results presented here will depend on the system size n_s , and our results for $n_s = 5$ may exaggerate the peak structure, but that the qualitative features are genuine. This is supported by comparison to quantum Monte Carlo results, the lack of any evident signature of finite size structure in our calculations, as well as the earlier findings of a similar peak feature in an independent study.¹³ Nevertheless, it is desirable to study larger system sizes within the present method to do a systematic finite size analysis. We hope that our results

will also motivate the development of methods that can achieve similarly high resolution at high energies to investigate this issue further.

We acknowledge informative discussions with Andrew Mitchell and valuable support from Hugo Strand and Stellan Östlund. We also thank Carsten Raas for providing the D-DMRG data from Karski et al.¹⁵. Support was provided by the Swedish Research Council (grant no. 2011-4054). Computations used resources at Chalmers Centre for Computational Science and Engineering (C3SE) provided by the Swedish National Infrastructure for Computing (SNIC).

1. Appendix: Perturbative motivation at large U

Here we demonstrate that the Dist-ED formalism applied to the Mott insulator may be motivated as a perturbation expansion in the small parameter $b_0 = 1 - a_0$, where a_0 is the weight of the $\omega = 0$ pole of the impurity-bath Greens function. To 0'th and 1'st order in b_0 , the method is exact to all orders in the standard perturbation expansion in U .

Consider an arbitrary n 'th order diagram in the expansion of the self-energy that contains $k = 2n - 1$ legs given by $G_0(z) = \frac{a_0}{z} + g_0(z)$, where the calculation consists of evaluating Matsubara sums of products of $G_0(i\omega_n)$ (or correspondingly real or imaginary frequency integrals.) Suppressing summations we can write a diagram schematically as $U^n(G_0)^k = U^n(a_0 + b_0)^k$ and expand in powers of b_0 (keeping in mind the underlying structure of summations that implies that the factors are not equivalent). We now want to study what approximation is made by calculating Σ as the sample average $\langle \Sigma^\nu \rangle = \frac{1}{N} \sum_{\nu=1}^N \Sigma^\nu$ where Σ^ν is the exact self energy of the finite size impurity problem. For simplicity we will consider the minimal 3-level system with impurity-bath Green's function $G_0^\nu = \frac{a_0}{z} + b_0(\frac{1/2}{z-b^\nu} + \frac{1/2}{z+b^\nu})$, where the pole locations b^ν are distributed according to $-\frac{1}{b_0\pi} \text{Im}g_0(w)$ such that $\langle G_0^\nu \rangle = \lim_{N \rightarrow \infty} \frac{1}{N} \sum_{\nu=1}^N G_0^\nu = G_0$.

The $(a_0)^k(b_0)^0$ term of the expansion corresponds to evaluating all the Green's function in terms of the $z = 0$ pole contribution. In the large U limit $a_0 \rightarrow 1$ and $b \rightarrow 0$ this corresponds to the Hubbard I approximation of an isolated site which is exact in this limit and which is obviously exactly represented by a finite system. To next order $(a_0)^{k-1}(b_0)^1$ we will use the second order diagram $\Sigma^{(2)} = U^2 \sum_{p,m} G_0(i\omega_{n-m})G_0(i\omega_p)G_0(i\omega_{m-p})$ ($\omega_n = \frac{\pi}{\beta}(2n + 1)$) for demonstration purpose but the proof would be analogous for an arbitrary self energy diagram. Thus evaluating terms proportional to $(a_0)^2 b_0$ we find

$$\begin{aligned}
\Sigma^{(2)}|_{a_0^2 b_0}/U^2 &= \sum_{p,m} G_0(i\omega_{n-m})G_0(i\omega_p)G_0(i\omega_{m-p})|_{a_0^2 b_0} \\
&= \sum_{p,m} \left(\frac{a_0}{i\omega_{n-m}} + g_0(i\omega_{n-m})\right) \left(\frac{a_0}{i\omega_p} + g_0(i\omega_p)\right) \left(\frac{a_0}{i\omega_{m-p}} + g_0(i\omega_{m-p})\right) |_{a_0^2 b_0} \\
&= \sum_{p,m} \left(\frac{a_0}{i\omega_{n-m}} \frac{a_0}{i\omega_p} g_0(i\omega_{m-p}) + \text{permutations of frequencies}\right). \tag{A.11}
\end{aligned}$$

This is to be compared to the corresponding expression in terms of a three level system,

$$\begin{aligned}
\Sigma_{\text{Dist-ED}}^{(2)}|_{a_0^2 b_0}/U^2 &= \left\langle \sum_{p,m} G_0^\nu(i\omega_{n-m})G_0^\nu(i\omega_p)G_0^\nu(i\omega_{m-p}) \right\rangle |_{a_0^2 b_0} \\
&= \left\langle \sum_{p,m} \left(\frac{a_0}{i\omega_{n-m}} + \frac{b_0}{2} \left(\frac{1}{i\omega_{n-m} - b^\nu} + \frac{1}{i\omega_{n-m} + b^\nu} \right) \right) \left(\frac{a_0}{i\omega_p} + \dots \right) \left(\frac{a_0}{i\omega_{m-p}} + \dots \right) \right\rangle |_{a_0^2 b_0} \\
&= \sum_{p,m} \left(\left(\frac{a_0}{i\omega_{n-m}} \frac{a_0}{i\omega_p} \left\langle \frac{b_0}{2} \left(\frac{1}{i\omega_{m-p} - b^\nu} + \frac{1}{i\omega_{m-p} + b^\nu} \right) \right\rangle \right) + \text{permutations of frequencies} \right) \\
&= \sum_{p,m} \left(\frac{a_0}{i\omega_{n-m}} \frac{a_0}{i\omega_p} g_0(i\omega_{m-p}) + \text{permutations of frequencies} \right) = \Sigma^{(2)}|_{a_0^2 b_0}/U^2, \tag{A.12}
\end{aligned}$$

where we have used the fact that b^ν are distributed according to $-Img_0$, which (using particle-hole symmetry) implies $\langle \frac{b_0}{z \pm b^\nu} \rangle = g_0(z)$. The demonstrated calculation clearly holds for any diagram implying that the Dist-Ed formalism is exact to 1'st order in b_0 . Nevertheless, for large U the self energy has pole strength $\alpha \sim U^2$,¹² giving $b_0 \sim 1/U^2$, such that regarded as expansion in $1/U$ the formalism is in fact only *exact* to order $1/U^2$, with higher order terms to all orders included systematically but approximately through the sample averaged exact diagonalization.

Going beyond first order, to order $(b_0)^2$, the representation in terms of finite systems will not be exact. It is clear, as expected, that larger finite systems will give better approximations. In fact, for a flat distribution ($Img_0(\omega) = \text{const.}$ in some interval) we expect that a representation in terms of five (or more) level systems will

be exact even to order $(b_0)^2$ because the calculation will give an unbiased sampling of two energies in the support of g_0 . The details of this however remain to be studied in greater depth.

The separation of the impurity-bath Greens function G_0 in a pole at $\omega = 0$ with a large fraction of the spectral weight and a gapped continuum is special to the insulator and not valid for the metallic solution. It is thus less clear-cut how to best sample the continuous Greens function in terms of finite systems. Although the Dist-ED method has been used successfully also for the metallic problem¹⁶ the original work used a rather ad-hoc method of discarding samples that overrepresented the low-energy spectral weight. How to best formulate the method for problems with continuous low-energy weight is still under investigation.

¹ J.W. Negele and H. Orland. *Quantum Many-Particle Systems* (Addison-Wesley, Reading, MA) 1988.

² N.F. Mott, *Metal Insulator Transitions* (Taylor and Francis, London) 1990.

³ A. George, G. Kotliar, W. Krauth, and M.J. Rozenberg, *Rev. Mod. Phys.* **68**, 13 (1996).

⁴ W. Metzner and D. Vollhardt, *Phys. Rev. Lett.* **62**, 324 (1989).

⁵ E. Müller-Hartmann, *Z. Phys. B Condensed Matter* **76**, 211 (1989).

⁶ A. Georges and G. Kotliar, *Physical Review B* **45**, 6479 (1992).

⁷ M. Jarrell, *Phys. Rev. Lett.* **69**, 168 (1992).

⁸ X. Y. Zhang, M. J. Rozenberg, and G. Kotliar. *Phys. Rev. Lett.* **70**, 1666 (1993).

⁹ M. Caffarel and W. Krauth, *Phys. Rev. Lett.* **72**, 1545 (1994).

¹⁰ D.E. Logan, M.P. Eastwood, and M.A. Tusk, *J. Phys.: Condens. Matter* **9**, 4211 (1997).

¹¹ R. Bulla, *Phys. Rev. Lett.* **83**, 136 (1999),

¹² E. Kalinowski and F. Gebhard, *Journal of Low Temp. Phys.* **126**, 979 (2002). M.P. Eastwood, F. Gebhard, E. Kalinowski, S. Nishimoto, and R.M. Noack, *Eur. Phys. J. B* **35**, 155 (2003).

¹³ S. Nishimoto, F. Gebhard and E. Jeckelmann, *J. Phys.: Cond. Mat.* **16**, 7063 (2004).

- ¹⁴ D.J. García, E. Miranda, K. Hallberg, M.J. Rozenberg, *Physica B: Condensed Matter* **398**, 407 (2007).
- ¹⁵ M. Karski, C. Raas, and G.S. Uhrig, *Phys. Rev. B* **77**, 075116 (2008).
- ¹⁶ M. Granath and H.U.R. Strand, *Phys. Rev. B* **86**, 115111 (2012).
- ¹⁷ Y. Lu, M. Höppner, O. Gunnarsson, and M. W. Haverkort, *Phys. Rev. B* **90**, 085102 (2014).
- ¹⁸ Martin Ganahl, Markus Aichhorn, Patrik Thunström, Karsten Held, Hans Gerd Evertz, Frank Verstraete, arXiv:1405.6728.
- ¹⁹ G. Sangiovanni, A. Toschi, E. Koch, K. Held, M. Capone, C. Castellani, O. Gunnarsson, S. K. Mo, J. W. Allen, H. D. Kim, et al., *Physical Review B* **73**, 205121 (2006).
- ²⁰ E. Jeckelmann *Phys.Rev.B* **66** 045114 (2002).
- ²¹ J.E. Hirsch and R.M. Fye, *Phys. Rev. Lett.* **56**, 2521 (1986).
- ²² Emanuel Gull, Andrew J. Millis, Alexander I. Lichtenstein, Alexey N. Rubtsov, Matthias Troyer, and Philipp Werner, *Rev. Mod. Phys.* **83**, 349 (2011).
- ²³ M. Ferrero and O. Parcollet, TRIQS: a Toolbox for Research in Interacting Quantum Systems, URL <http://ipht.cea.fr/triqs>.